


Article

Effect of Carbon Content on the Microstructure and Mechanical Properties of NbC-Ni Based Cermets

Shuigen Huang ^{1,*} , Patrick De Baets ², Jacob Sukumaran ², Hardy Mohrbacher ³, Mathias Woydt ⁴ and Jozef Vleugels ¹

¹ Department of Materials Engineering (MTM), KU Leuven, Kasteelpark Arenberg 44, B-3001 Heverlee, Belgium; jozef.vleugels@kuleuven.be

² Department of Mechanical Construction and Production, Ghent University, Technologiepark 903, 9052 Zwijnaarde, Belgium; Patrick.DeBaets@UGent.be (P.D.B.); JacobPremKumar.Sukumaran@UGent.be (J.S.)

³ NiobelCon bvba, B-2970 Schilde, Belgium; niobelcon@skynet.be

⁴ BAM Federal Institute for Materials Research and Testing, Division 6.3 Tribology & Wear Protection, Unter den Eichen 44-46, D-12203 Berlin, Germany; mathias.woydt@bam.de

* Correspondence: shuigen.huang@kuleuven.be; Tel.: +32-16-321-777

Received: 11 January 2018; Accepted: 6 March 2018; Published: 12 March 2018

Abstract: The aim of this work was to correlate the overall carbon content in NbC-Ni, NbC-Ni-VC and NbC-Ni-Mo starting powders with the resulting microstructure, hardness, and fracture toughness of Ni-bonded NbC cermets. A series of NbC-Ni, NbC-Ni-VC and NbC-Ni-Mo cermets with different carbon content were prepared by conventional liquid phase sintering for 1 h at 1420 °C in vacuum. Microstructural analysis of the fully densified cermets was performed by electron probe microanalysis (EPMA) to assess the effect of carbon and VC or Mo additions on the NbC grain growth and morphology. A decreased carbon content in the starting powder mixtures resulted in increased dissolution of Nb, V, and Mo in the Ni binder and a decreased C/Nb ratio in the NbC based carbide phase. The Vickers hardness (HV₃₀) and Palmqvist indentation toughness were found to decrease significantly with an increasing carbon content in the Mo-free cermets, whereas an antagonistic correlation between hardness and toughness was obtained as a function of the Mo-content in Mo-modified NbC cermets. To obtain optimized mechanical properties, methods to control the total carbon content of NbC-Ni mixtures were proposed and the prepared cermets were investigated in detail.

Keywords: niobium carbide; cermet; hardmetal; liquid phase sintering; carbon; hardness

1. Introduction

WC-Co cemented carbides are widely used hard materials for cutting tools and wear applications. To improve the sintering behavior, refine the carbide grain size, and fine tune the mechanical properties, transition metal carbides, such as VC, Cr₃C₂, NbC, TaC, and Mo₂C, are commonly added in small quantities to WC-Co cemented carbides [1–3] and in larger fractions to TiCN–Ni based cermets [4–7]. Compared to WC and Ti(C,N), NbC has a higher melting point (3522 °C) and is, on average, softer [8]. The good retention of hot hardness of NbC closes the gap at 800 °C to WC. NbC has a low density (7.79 g/cm³), comparable to steel, and a good chemical stability of Nb₂O₅ against water. Despite the promising properties of NbC, the potential of NbC as a major component in hard materials for wear applications was only recently reported by Woydt et al. [9,10] and for machining by Uhlmann et al. [11]. A remarkable NbC grain growth was observed in Co and Ni bonded NbC cermets after liquid phase sintering [12,13]. The NbC grains formed an interconnected network and a combined trans/inter-granular fracture mode was detected on fracture surfaces. To control the NbC grain growth and improve the densification behavior, transition metal carbides, such as VC, TiC,

WC and Mo₂C were recently reported to be very efficient to control the microstructure of NbC-Ni or NbC-Co based cermets [14,15]. The NbC grain growth was significantly inhibited and a homogeneous NbC grain size distribution was obtained upon liquid phase sintering of the transition metal carbides modified NbC cermets.

Monocarbides of transition metals have a wide homogeneity range and preserve their NaCl structure in the presence of vacancies in the carbon sublattice. A variation in the concentration of these vacancies strongly affects the properties of the monocarbides. According to Ramqvist [16] and Vinitskii [17], the microhardness directly characterizes the bond strength. The hardness of cubic carbides TiC, ZrC, HfC, and VC increase with increasing combined carbon in the carbides, whereas the hardness of pure NbC and TaC reaches a maximum at a C/Me atomic ratio of 0.80 [16]. The HV_{0.05} of NbC decreases significantly from 3300 to 1500 kg/mm² when the C/Nb ratio is increased from 0.75 to 1.0 [17]. In a metal bonded cubic carbide/nitride cermet system, the carbon content not only influences the hardness of the hard carbide/nitride phase, but also the grain size and morphology of the hard phase, as well as the composition of the binder phase. The carbon content in WC-Co materials plays an important role with respect to the WC grain growth and binder composition as well as the phase constitution. A low carbon content in the WC-Co system leads to finer-grained WC grains and increased W concentration in the Co binder [18]. In Mo₂C or WC modified Ti(C,N)-Ni cermets, the carbon content has an influence on the stability of the carbide and nitride [19,20]. A higher carbon addition decreases the dissolution of W, Ti, and Mo in the binder phase, whereas a lower carbon content resulted in aggregation of the ceramic grains due to the fact that they are poorly wetted by the liquid metal during sintering [21]. A carbon deficient brittle eta phase or free graphite phase was reported when the carbon content was not well controlled [22]. In this study, NbC-Ni based cermets with VC or Mo additions were prepared from NbC starting powders with a different carbon content. The goal was to investigate the influence of the carbon content in the NbC starting powder on the microstructure and mechanical properties of NbC-Ni based cermets, as well as the NbC-Ni based cermets with VC and Mo additions.

2. Experimental

2.1. Materials Preparation

Two NbC grades (NbC-A and NbC-B), Ni (Vale, T123TM, FSSS = 3–7 μm, Prescott, UK), VC (Langfeng, FSSS = 3.38 μm, Changsha, China), Mo (Plansee, 3–5 μm, Reutte, Austria), NbH₂ (CBMM, AD-5882, 40 μm, Araxa, Brazil) as well as carbon black (Degussa, Grade 4, Hanau, Germany) powders were used to prepare NbC-Ni based cermets. The Co and O content of the Ni powder are less than 0.00005 and 0.04 wt %, respectively. The VC powder has a total C of 18.08 wt % and O of 0.32 wt %. The Mo powder contains an O impurity of 0.4 wt %. The total carbon content in the NbC-A and B powders is 11.2 and 12.3 wt %, whereas the O content is 0.28 and 0.37 wt %, respectively, as listed in Table 1. Free graphite is expected in the NbC-B powder since the maximum combined carbon in a pure NbC (C/Nb = 1) is 11.45 wt %.

Table 1. Some characteristics of NbC starting powders.

Powder	Density (g/cm ³)	Particle Sized ₅₀ (μm)	Total C Content(wt %)	Total O Content(wt %)
NbC-A	7.71	9.4	11.2	0.28
NbC-B	7.46	6.9	12.3	0.37

The microstructure of the two NbC starting powders and metal powders Mo and Ni are shown in Figure 1. Both the NbC powders contain sub-micron sized primary NbC particles. Most of the Mo particles in Figure 1c are of spherical shape. The fine fraction of Mo particles is less than 1 μm. The fine

fraction Mo particles tend to form clusters. The Ni powder, as shown in Figure 1d, contains 4–8 μm Ni powder agglomerates.

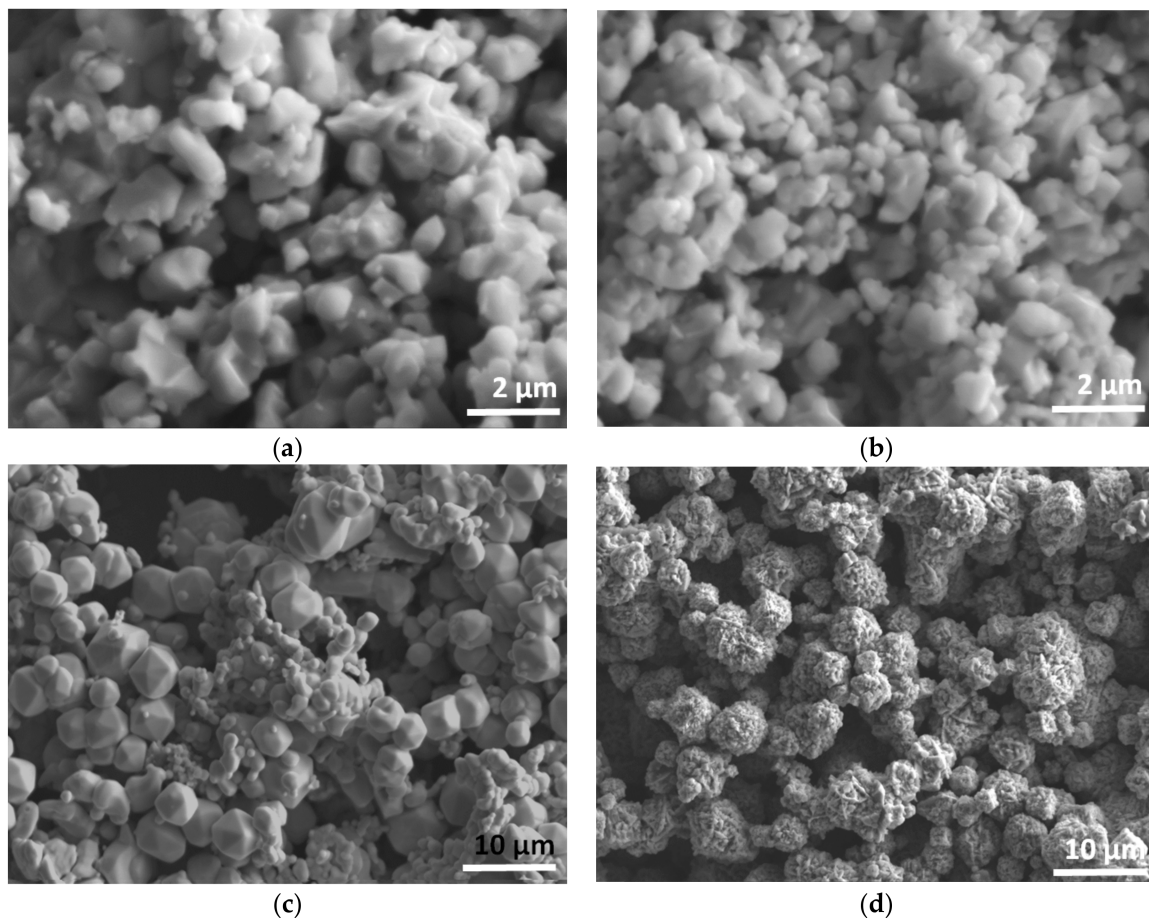


Figure 1. Morphology of the NbC starting powders, (a) NbC-A (11.2 wt % C) and (b) NbC-B (12.2 wt % C), (c) Mo powder and (d) Ni powder.

As summarized in Table 2, three series of experiments were designed to investigate the role of C on the properties of NbC-Ni cermets. The calculated overall carbon content in the (NbC + C + NbH₂ + VC/Mo) starting powders is summarized in Table 2. The addition of NbH₂ or C was intended to change the carbon content of the powder mixtures. Initially, the influence of NbH₂ and C addition on the microstructure and properties of NbC-12 vol % Ni cermets was investigated. Up to 4 vol % NbC was substituted by NbH₂ or C, whereas the Ni content was fixed at 12 vol %. A second series of experiments was performed to elucidate the effect of the C content on the properties of NbC-12 vol % Ni cermets with 5 vol % VC addition. 5 vol % VC was added into the system to control the NbC grain growth and to enhance the hardness and fracture toughness. In a finale set of experiments, a carbon-rich NbC starting powder (grade NbC-B) was mixed with 12 vol % Ni and 0–15 vol % Mo. The total carbon content of the Mo containing powder mixtures is decreased with increasing replacement of NbC by Mo metal. Mo is added to react with the free carbon from the NbC starting powder and to refine the NbC grain size. The powder mixtures were mixed on a multi-directional mixer (Turbula, WAB, Muttenz, Switzerland) in ethanol for 24 h using WC-6 wt % Co milling balls (Ceratzit grade H20C, Ø10 mm). The suspension was dried in a rotating evaporator at 65 °C. Cold isostatically pressed (200 MPa) powder compacts (Ø20 mm × 10 mm) were conventional pressureless sintered for 1 h at 1420 °C in a dynamic vacuum (~20 Pa) with a heating rate of 10 °C/min in a resistively graphite heating element furnace.

Table 2. Chemical composition of the investigated NbC-Ni based cermets.

Experimental Goal	Composition (vol %)	Calculated C in Carbide (wt %)	Starting Powders
Influence of C on NbC-12 vol % Ni cermets	(NbC-4NbH ₂)-12Ni	10.82	NbC-A, Ni, NbH ₂ , C
	(NbC-2NbH ₂)-12Ni	11.01	
	NbC-12Ni	11.20	
	(NbC-2C)-12Ni	11.72	
	(NbC-4C)-12Ni	12.26	
Influence of C on NbC-12 vol % Ni-5 vol % VC cermets	(NbC-4NbH ₂)-5VC-12Ni	11.11	NbC-A, Ni, NbH ₂ , C
	(NbC-2NbH ₂)-5VC-12Ni	11.30	
	NbC-5VC-12Ni	11.50	
	(NbC-2C)-5VC-12Ni	12.03	
Influence of Mo on C-rich NbC-12 vol % Ni cermets	NbC-12Ni	12.20	NbC-B, Ni, Mo
	(NbC-5Mo)-12Ni	11.41	
	(NbC-10Mo)-12Ni	10.64	
	(NbC-15Mo)-12Ni	9.90	

2.2. Characterization

The bulk density of the sintered cermets was measured in ethanol. The sintered materials were cross-sectioned, ground with 15 μm diamond suspension, followed by polishing steps using 3 and 1 μm diamond suspension. The mechanically polished surfaces were then further polished with colloidal SiO₂ suspension for 10 min to yield a stress-free surface. Microstructure analysis and composition analysis of the carbide grains of polished cermets was performed by electron probe microanalysis (EPMA, JXA-8530F, JEOL Ltd., Tokyo, Japan). Phase identification on polished surfaces was conducted by a θ - θ X-ray diffractometer (XRD, Seifert 3000, Ahrensburg, Germany) using Cu K α radiation (40 kV, 40 mA). The lattice parameters of the carbide and binder phases were calculated based on the XRD patterns. The Vickers hardness, HV₃₀, was measured on a hardness tester (Model FV-700, Future-Tech Corp., Tokyo, Japan) under an indentation load of 30 kg for 15 s. The Palmqvist indentation toughness, K_{IC}, was calculated from the length of the radial cracks around the Vickers HV₃₀ indentations, according to a formula proposed by Shetty et al. [23]. The reported values are the mean and standard deviation of five indentations.

3. Results and Discussion

3.1. Influence of Carbon Content in NbC-12 vol % Ni Cermets

Backscattered electron micrographs (BSE) of liquid phase sintered NbC-12 vol % Ni cermets with different carbon content are shown in Figure 2. Based on the image and density measurement, all the cermets were fully densified. The bright and dark-grey contrast grains correspond to the NbC and Ni binder, respectively. The dark contrast grains in the C-rich cermet in Figure 2e is confirmed to be free graphite grains. A small fraction of Nb oxide was found in the NbC grains due to the rapid NbC grain growth. It is clear that the morphology and particle size of the NbC grains, as well as the wetting between NbC and Ni binder were evolved as a function of the carbon content. During liquid phase sintering, the growth of NbC grains in a Co, Ni, or Fe binder was reported to be a result of dissolution and re-precipitation [24]. For the Nb-rich (low carbon) cermets with 2 and 4 vol % NbH₂ additions (see Figure 2a,b), most of the coarser NbC grains have a clear rounding of the edges, while the small grains are almost spherical. In the C-rich NbC cermets, the grains are more faceted and triangular prisms with sharp corners appear, as shown in Figure 2d,e. Although NbC has a different crystal structure than WC, there exists a similar trend in carbide morphology evolution with the C content in the sintered materials. In a W-rich WC-Co material, the WC grains have slightly rounded corners, whereas more faceted and truncated grains are common in C-rich WC-Co materials [18]. The sintered NbC-12 vol % Ni cermet (Figure 2c) had substantially larger NbC grains compared to the grades with NbH₂ or C addition. The NbC grain size in the two low carbon cermets is found to be smaller compared to the C-added cermets. On the other hand, wetting of the Ni binder and NbC grains is improved

with increasing carbon content. The improved wetting can be due to the removal of residual oxides from NbC (0.28 wt % O in NbC) and Ni in the starting powders by means of carbothermal reduction during sintering. The oxide layer on the surface of NbC and Ni grains can reduce the surface energy of the carbide and binder phases [21]. With increasing C content, the residual oxides were completely reduced, therefore increasing the surface energy of the carbide grains, resulting in a decreased wetting angle between binder and carbide phase.

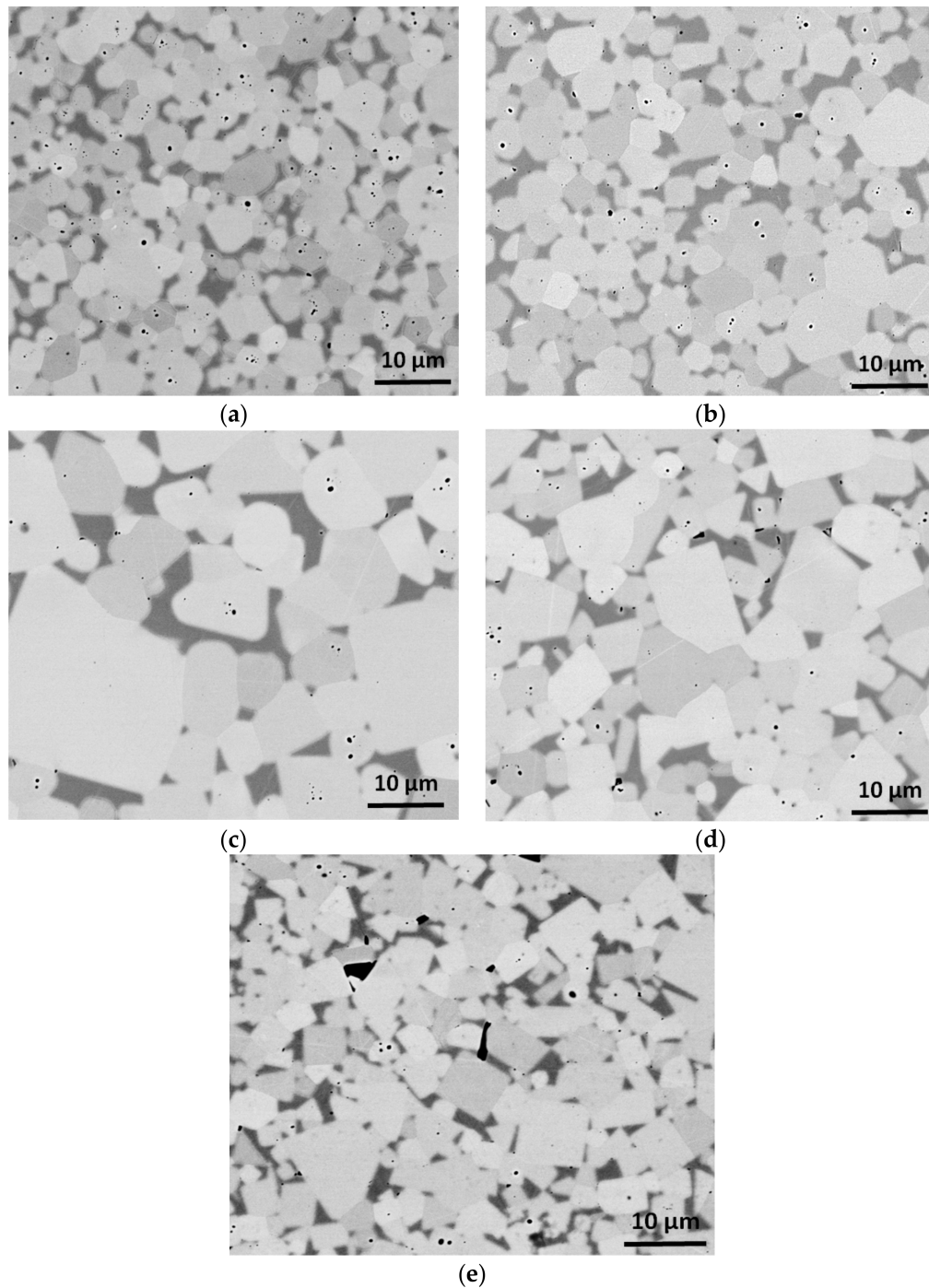


Figure 2. Influence of carbon content on the microstructure of the NbC-12 vol % Ni based cermets sintered for 1 h at 1420 °C. (a) (NbC-4NbH₂)-12Ni, (b) (NbC-2NbH₂)-12Ni, (c) NbC-12Ni, (d) (NbC-2C)-12Ni and (e) (NbC-4C)-12Ni.

XRD phase analysis, as shown in Figure 3a, confirmed that all sintered cermetes are composed of a fcc solid solution Ni binder and a cubic solid solution NbC phases. No residual NbH₂, Nb, or C phases were observed by XRD in the sintered cermetes. During sintering, complete decomposition of NbH₂ into Nb and H₂ was reported to be below 500 °C, whereas the densification of the powder compacts had not started [25]. The generated H₂ was therefore removed from the powder compact under vacuum atmosphere. The C and metallic Nb can dissolve both in the binder and carbide phases, depending on the C content in the binder phase. The higher the C content in the binder, the lower the expected Nb concentration is in the binder. As shown in Figure 3a, the diffraction peaks of the NbC phase slightly shifted toward lower angle with increased C content in the cermetes, indicating that a higher C content in the NbC phase. On the other hand, the peaks of the Ni binder phase shifted toward higher angle with increased C content. The measured lattice parameters of the NbC and Ni phases are plotted as a function of the NbH₂ and carbon addition in Figure 3b. With increasing C content, the lattice parameter of the NbC phase increased, whereas the lattice parameter of the Ni binder decreased. For binderless NbC, the lattice parameter of the cubic NbC phase is related to its carbon content, i.e., the higher the carbon content, the larger the lattice parameter [26]. Since Ni is not found in the NbC grains, the change in lattice parameter of the NbC phase is only due to a varied carbon or Nb content. The addition of C to the cermetes increased, whereas the addition of NbH₂ reduced the C content of the NbC phase. Regarding the Ni binder, the decreased lattice parameter with increasing overall carbon content is due to a decreased Nb solubility in the binder. The atomic radius of Nb is larger than Ni. Therefore, the larger the lattice parameter of the Ni binder, the higher the concentration of dissolved Nb in Ni binder. Comparing the lattice parameters of the NbC and Ni starting powders with that of the sintered NbC-12 vol % Ni cermet reveals a loss of carbon in the NbC phase and the dissolution of Nb in the Ni binder during sintering. With the addition of C or NbH₂, the redistribution of Nb and C in the Ni binder and NbC phases became more pronounced. The XRD analysis clearly indicates that the C/Nb ratio of the NbC phase in the Ni bonded cermetes can be modified with the addition of C or Nb.

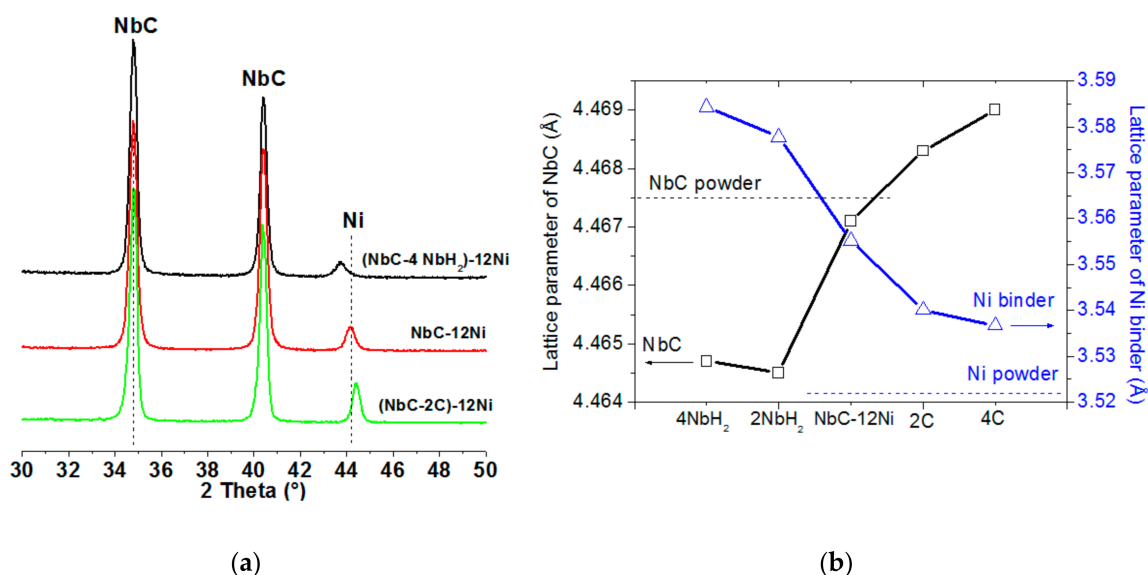


Figure 3. X-ray diffractometer (XRD) patterns of the NbC-12 vol % Ni cermetes with different C content (a) and influence of the C content on the lattice parameter of NbC and Ni binder phases (b).

To verify this hypothesis, a thermodynamic evaluation was done using Thermo-Calc software [27] in combination with the commercial database TCNI8. The calculated isothermal section of the Ni-Nb-C ternary system at 1420 °C is shown in Figure 4a, clearly indicating that the chemical composition of the liquid Ni binder depends on the carbon content of the NbC phase. The C-rich liquid binder

is in equilibrium with a C-rich $\text{NbC}_{1.0}$ phase. With decreasing C content, the concentration of Nb is increased in the liquid binder, whereas the C content of the equilibrium NbC phase is reduced. The observed phase constitution in the sintered cermet was verified in the calculated phase diagram, as shown in Figure 4b. The cermet with up to 4 vol % NbH_2 addition are in the NbC + Ni two phases region after cooling from the sintering temperature, whereas the 2 vol % C added cermet is located in the area where the stable phases are NbC, Ni, and graphite. The extra graphite phase was not observed by XRD analysis in the C added cermet due to their low content.

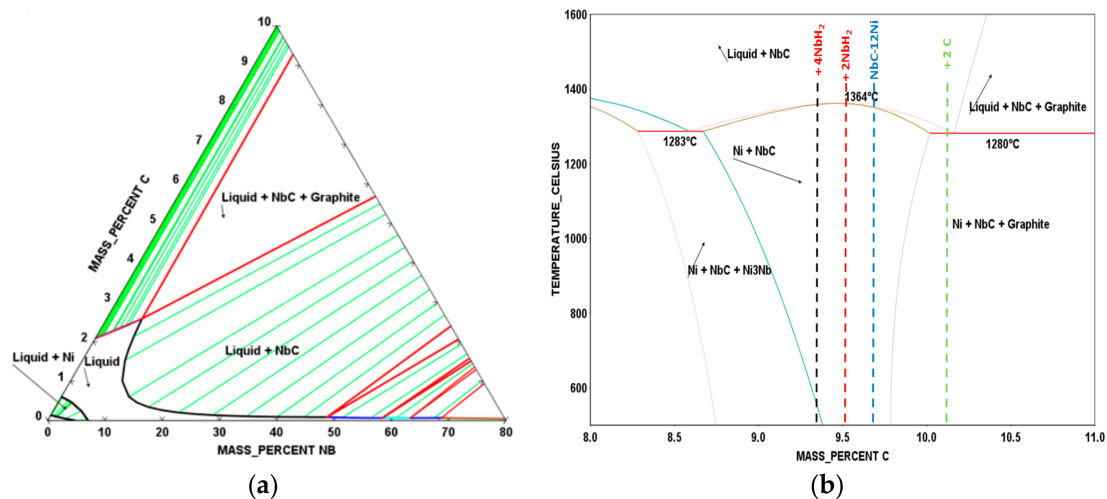


Figure 4. Calculated isothermal section of Ni-Nb-C system at 1420 °C (a) and influence of the C content on the phase relation of the Nb-C-12 vol % Ni system (b).

3.2. Influence of the Carbon Content in NbC-12 Ni-5 VC (vol %) Cermet

It was reported that rapid NbC grain growth in Ni bonded NbC cermet could be controlled with the addition of VC or Mo_2C , therefore to improve mechanical properties [10]. Figure 5 shows the BSE images of fully densified NbC-12Ni-5VC (vol %) cermet with different C contents. Similar to the NbC-12 vol % Ni cermet, the VC modified cermet also have a simple two phases, i.e., a bright grey NbC and dark grey Ni binder. Individual VC grains are not detected in the microstructure. The NbC grains form an interconnected skeleton and the binder phase is distributed homogeneously in the NbC matrix. The shape of the large NbC grains is well-faceted with a slight rounding of the edges, while the small grains are almost spherical. Compared to the microstructure of the NbC-12 vol % Ni cermet (Figure 2c), the most obvious effect of the VC addition is a significantly reduced NbC grain size. Most of the NbC grains are below 10 μm , as shown in (Figure 5a–c). However, with the addition of 2 vol % C, the NbC grain size increased significantly again and the contiguity of the NbC phase decreased. The growth behavior of the NbC grains is therefore not only dependent on the secondary carbide addition, but also on the combined carbon content. The grain growth inhibiting effect of VC (<1 wt %) addition has been reported for a number of WC-Co cemented carbides [18] and is of common industrial practice. Theories on the WC grain growth inhibition assume either an alteration of the interfacial energy or an interaction of the inhibitors with the WC grain dissolution/re-precipitation process. The higher the availability of VC, the larger the potential effect on the interfacial free energy and the more pronounced the suppression of WC grain growth [28,29]. In the VC modified NbC-Ni cermet, a mixed carbide (Nb,V)C is formed during sintering [15]. The composition of the binder is also changed since VC has a much higher solubility in Ni, as compared to NbC [30]. The surface energy of the liquid Ni binder and the NbC grains is changed during sintering, therefore affecting the NbC grain growth behavior.

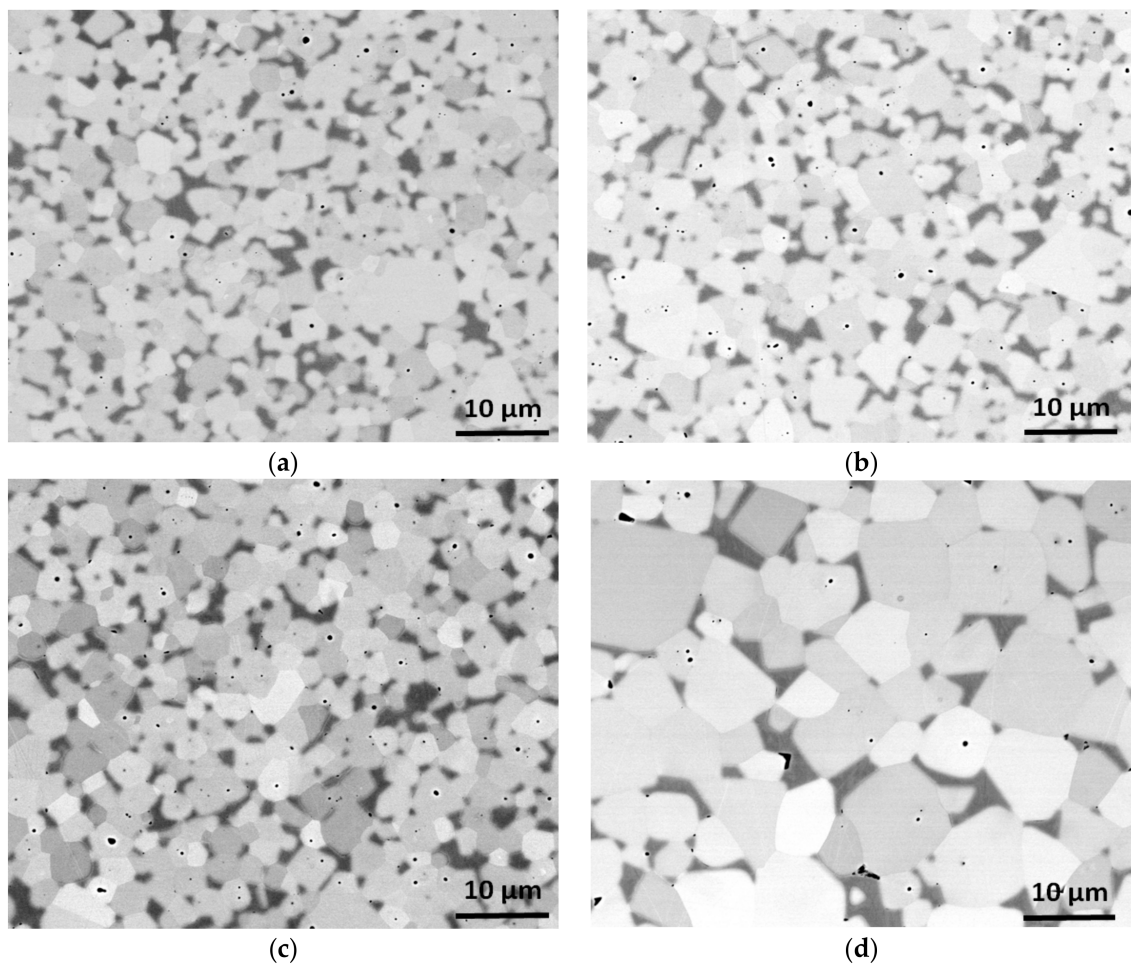


Figure 5. Influence of carbon content on the microstructure of 5 vol % VC modified NbC-12 vol % Ni cermet sintered for 1 h at 1420 °C. (a) (NbC-4NbH₂)-5VC-12Ni, (b) (NbC-2NbH₂)-5VC-12Ni, (c) NbC-5VC-12Ni, (d) (NbC-2C)-5VC-12Ni (vol %).

The phase analysis from XRD patterns indicated all sintered cermets are composed of a fcc solid solution Ni binder and cubic solid solution (Nb,V)C phase, as shown in Figure 6a. The lattice parameter of the cubic (Nb,V)C and Ni binder in the 12 vol % Ni bonded cermets are plotted in Figure 6b. Compared to the NbC starting powder and NbC-12Ni cermets, the dissolution of VC into the NbC phase resulted in a clearly decreased unit-cell since the atomic radius of V is smaller than that of Nb. The dissolution of V in NbC grains was also confirmed by energy dispersive spectrometer (EDS) analysis. The concentration of V in NbC grains is increased with increasing C content, from 2.75 wt % V in the (NbC-4NbH₂)-5VC-12Ni (vol %) cermet to 3.69 wt % V in the (NbC-2C)-5VC-12Ni (vol %) cermet. The influence of the C content on the lattice parameters of NbC and Ni phases are similar as for the NbC-Ni cermets (Figure 3). With increasing carbon addition, the lattice parameter of (Nb,V)C gradually increased, whereas the lattice parameter of the Ni binder decreased indicating that the dissolution of V and Nb in the Ni binder decreased with increasing carbon content.

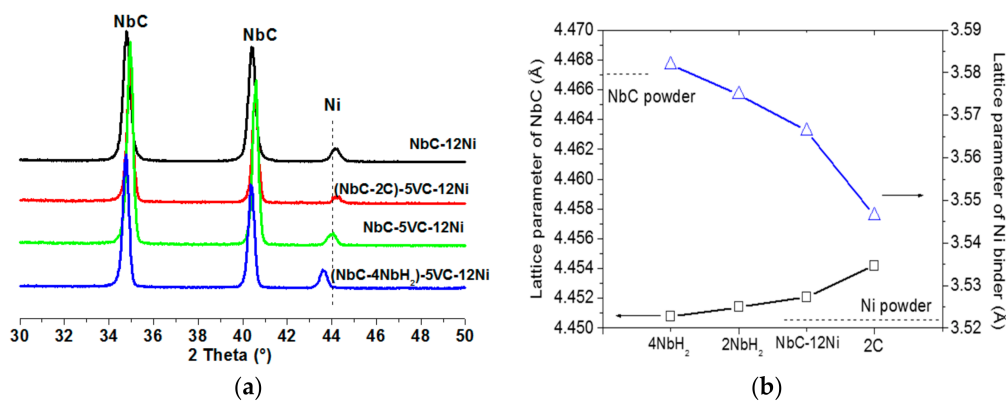


Figure 6. Influence of C content on the XRD phase patterns (a) and lattice parameter (b) of NbC and Ni binder phases in the 5 vol % VC modified NbC-12 vol % Ni cermet.

The hardness and indentation toughness of the two series cermet are plotted as a function of the estimated NbC_x stoichiometry in Figure 7. The x value is estimated based on the overall carbon content of the starting powder compositions. Generally, the hardness of the cermets decreased with increasing C content. The lowest hardness was found in the cermet saturated with free graphite. As described earlier, the increased hardness can be directly linked to the intrinsic hardness of the NbC_x phase and the NbC grain size. With 5 vol % VC content, the red line in Figure 7a indicates the maximum hardness of 1356 kg/mm² in the 4 vol % NbH₂ cermet and the minimum hardness of 1004 kg/mm² in the C rich cermet. As compared to the NbC-12 vol % Ni cermets, a significant increase in hardness of nearly 100–300 kg/mm² was found in the cermets with 5 vol % VC addition, which can be directly linked to the refined NbC grain size and the formation of a (Nb,V)C solution carbide. However, the influence of VC on the hardness of (Nb,V)C is not known in this study. Without VC addition, a maximum toughness was found for the cermets with the lowest carbon content, i.e., the cermets with 4 vol % NbH₂ addition. With the addition of VC, both the 2 vol % NbH₂ and reference NbC-12Ni-5VC (vol %) cermets exhibit a high toughness around 11.5 MPa m^{1/2}, whereas the 4 vol % NbH₂ and 2 vol % C added cermets have a lower toughness value of 9.77 and 10.37 MPa m^{1/2}, respectively. According to the indentation crack propagation pattern, it is found that the cracks are mainly propagated along the carbide and binder grain boundaries in the VC added cermets, whereas trans-granular fracture of NbC grains is the major crack propagation pattern in the VC free cermets. It is worth to note that the optimum addition of NbH₂ is dependent on the carbon content of the NbC starting powder.

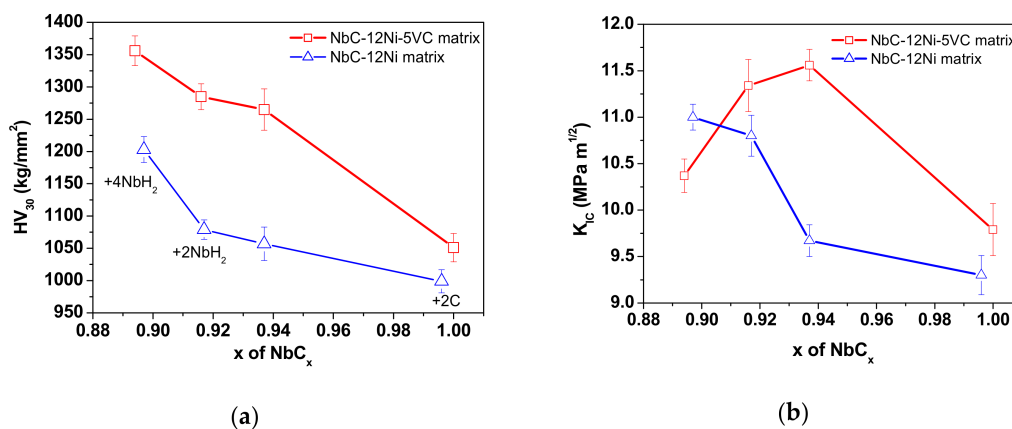


Figure 7. Mechanical properties of the NbC-12 vol % Ni and NbC-5 vol % VC-12 vol % Ni based cermets, (a) Vickers hardness (HV₃₀) and (b) Indentation fracture toughness (K_{IC}).

3.3. Influence of Mo Content in Carbon-Rich NbC-12 vol % Ni Cermets

Mo or Mo₂C is usually added into TiC or TiCN based cermets to improve the wetting and refine the ceramic grain size [5,7]. In this study, the goal of Mo addition into a carbon-rich NbC-12 vol % Ni system was to decrease the total carbon content and to evaluate its influence on mechanical properties. Figure 8 shows the BSE images of four fully densified NbC cermets with 12 vol % Ni binder and different Mo contents, obtained by liquid phase sintering for 1 h at 1420 °C in vacuum. The NbC-B grade starting powder contains 0.8 wt % free carbon. As shown in Figure 8a,b, dark contrast graphite grains can be found in the cermets without and with 5 vol % Mo addition. With increasing Mo content up to 10 and 15 vol %, all the graphite grains disappeared and a fine NbC grain (<5 μm) microstructure was obtained. No metallic Mo and Mo₂C were detected in these cermets. It is clear that Mo reacted with the free carbon to form a mixed (Nb,Mo)C during sintering. Like the NbC-12 Ni-5 VC cermets, the Mo-modified cermets also have a simple two-phase structure, i.e., NbC and Ni binder, even with 15 vol % Mo addition. In TiCN-based cermets, Mo or Mo₂C is usually added to refine the ceramic grains [4–7]. Core-rim carbonitride grains are commonly reported for these cermets, with a Mo-enriched rim area and Mo-rich Ni binder phase. In this study, the NbC grains of the 10 and 15 vol % modified cermets have a homogeneous contrast, indicating that a core-rim structure is not formed when Ti-rich carbide or nitride is not presented.

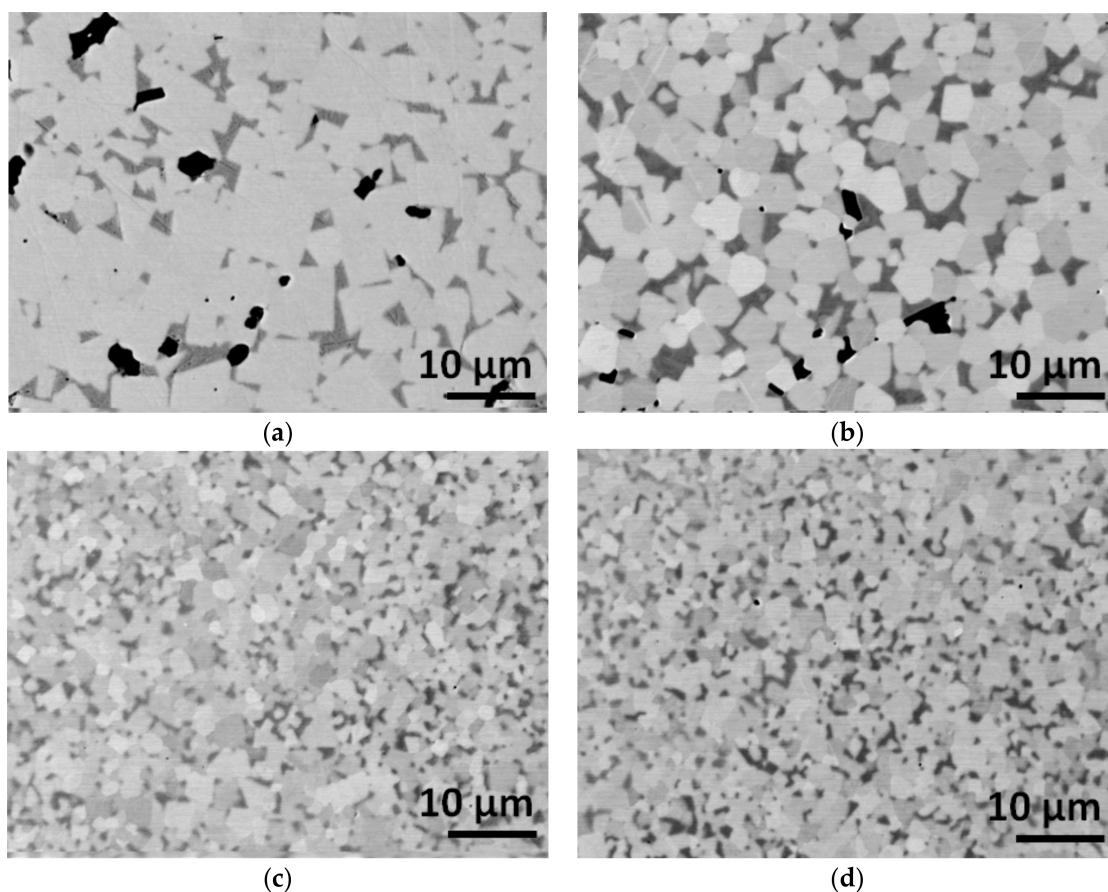


Figure 8. Influence of Mo content on the microstructure of NbC-12 vol % Ni based cermet sintered for 1 h at 1420 °C. (a) NbC-12Ni, (b) (NbC-5Mo)-12Ni, (c) (NbC-10Mo)-12Ni, (d) (NbC-15Mo)-12Ni cermet.

The evolution of the lattice parameters of the Mo-containing cermets explains the redistribution of Mo after sintering of the carbon-rich NbC powder with Mo and Ni binder. With increasing Mo content, the lattice parameter of the NbC phase decreased, whereas the lattice constant of the Ni

binder increased, as shown in Figure 9a. Since Ni was not found in the NbC phase, the decreased lattice parameter of the NbC phase is mainly due to the dissolution of Mo and C into NbC and formation of a mixed carbide (Nb,Mo)C. With decreasing carbon content in the starting powder mixtures via the increased addition of Mo, the dissolution of Mo into the Ni binder resulted in an increased unit-cell of the binder phase. Based on point analysis of the carbide and Ni binder, the Ni binder exhibited a higher solubility of Mo than the carbide phase.

The hardness and indentation toughness of the Mo modified cermets are plotted in Figure 9b. As expected from the NbC grain size evolution, the hardness of the cermets increased significantly with increasing replacement of NbC by Mo. The increased hardness is due to the reduced NbC grain size, the formation of solid solution (Nb,Mo)C carbides, as well as the decreased carbon content in the mixed carbide [16]. A significant increase in hardness of nearly 600 kg/mm² was observed in the cermet with 15 vol % Mo addition, as compared to the reference NbC-12 Ni cermet, using the C-rich NbC starting powder. Regarding the fracture resistance, a maximum toughness was found for the cermet without Mo addition, which decreased gradually with increasing Mo content. A good combination of hardness and toughness was found in the cermet with 15 vol % Mo addition, i.e., a HV₃₀ of 1466 kg/mm² and a fracture resistance of 8.2 MPa m^{1/2}.

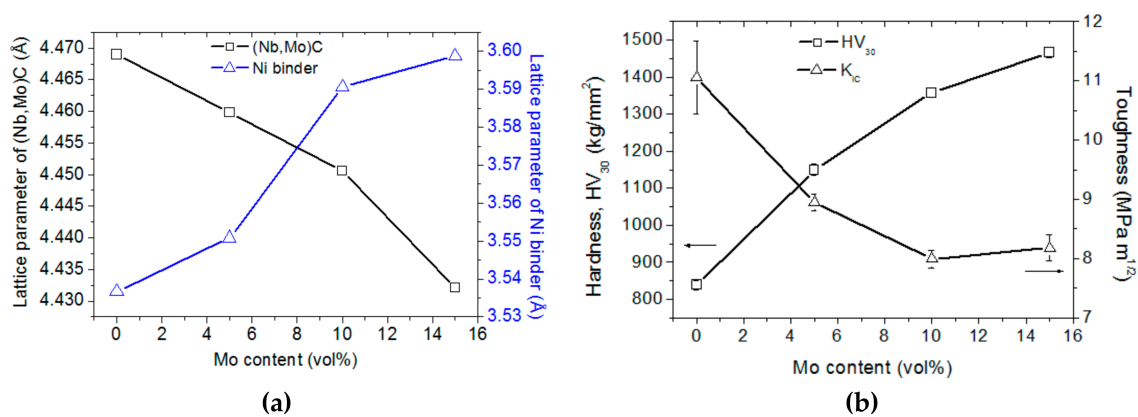


Figure 9. Influence of Mo addition on the lattice parameters of the carbide (square symbol) and binder phases (triangle symbol) (a) and mechanical properties (b) of (NbC-*x* vol % Mo)-12 vol % Ni cermets.

4. Conclusions

Full densification of 12 vol % Ni-bonded NbC-based cermets with different C contents and VC or Mo addition was achieved by pressureless liquid phase sintering in vacuum for 1 h at 1420 °C. All the cermets are composed of a fcc solid solution Ni binder and a cubic NbC, (Nb,V)C or (Nb,Mo)C solid solution phase.

The C content of the NbC starting powder has a significant impact on the microstructure and mechanical properties of NbC-Ni based cermets. The addition of 5 vol % VC significantly improved the hardness of NbC-Ni cermets, without clearly decreasing the toughness. The solubility of VC into NbC and Ni phases is closely related to the total carbon content of the NbC-Ni powder mixtures. The higher the C content, the lower the solubility of V and Nb in the Ni binder, and the higher the C content in the NbC or (Nb,V)C phase.

The addition of metallic Mo to C-rich NbC-Ni mixtures allowed to decrease the free C content of NbC and reduce the carbide grain size, resulting in an increased hardness but decreased fracture resistance. The Mo content in the Ni-binder and (Nb,Mo)C grains increased with increasing Mo addition.

Acknowledgments: We gratefully acknowledge the support of the Companhia Brasileira de Metalurgia e Mineração (CBMM), São Paulo, Brazil. The authors thank the Hercules Foundation (project ZW09-09) and the Fund for Scientific Research Flanders (FWO) under project G.0772.16N.

Author Contributions: Shuigen Huang, Jozef Vleugels and Mathias Woydt contributed to the design and implementation of the research, to the analysis of the results and to the writing of the manuscript. Jozef Vleugels, Patrick De Baets, Jacob Sukumaran and Hardy Mohrbacher helped supervise the project.

Conflicts of Interest: The authors declare no conflict of interest.

References

1. Bock, A.; Schubert, W.D.; Lux, B. Inhibition of Grain Growth on Submicron Cemented Carbides. *Powder Metall. Int.* **1992**, *24*, 20–26.
2. Sadangi, R.K.; McCandlish, L.E.; Kear, B.H.; Seegopaul, P. Grain Growth Inhibition in Liquid Phase Sintered Nanophase WC/Co Alloys. *Int. J. Powder Met.* **1999**, *35*, 27–33.
3. Wittmann, B.; Schubert, W.D.; Lux, B. WC Grain Growth and Grain Growth Inhibition in Nickel and Iron Binder Hardmetals. *Int. J. Refract. Met. Hard Mater.* **2002**, *20*, 51–60. [[CrossRef](#)]
4. Delannay, F.; Froyen, L.; Deruyttere, A. The Wetting of Solids by Molten Metals and its Relation to the Preparation of Metal-Matrix Composites. *J. Mater. Sci.* **1987**, *22*, 1–16. [[CrossRef](#)]
5. Zhang, S. Titanium Carbonitride-Based Cermets: Processes and Properties. *Mater. Sci. Eng. A* **1993**, *163*, 141–148. [[CrossRef](#)]
6. Ahn, S.Y.; Kim, S.W.; Kang, S. Microstructure of Ti(CN)-WC-NbC-Ni Cermets. *J. Am. Ceram. Soc.* **2001**, *84*, 843–849. [[CrossRef](#)]
7. Peng, Y.; Miao, H.Z.; Peng, Z.J. Development of TiCN-Based Cermets: Mechanical Properties and Wear Mechanism. *Int. J. Refract. Met. Hard Mater.* **2013**, *39*, 79–89. [[CrossRef](#)]
8. Pierson, H.O. *Handbook of Refractory Carbides and Nitrides*; William Andrew: Noyes, NJ, USA, 1996.
9. Woydt, M.; Mohrbacher, H. The Tribological and Mechanical Properties of Niobium Carbides (NbC) Bonded with Cobalt or Fe₃Al. *Wear* **2014**, *321*, 1–7. [[CrossRef](#)]
10. Huang, S.G.; Vleugels, J.; Mohrbacher, H.; Woydt, M. Microstructure and Tribological Performance of NbC-Ni Cermets Modified by VC and Mo₂C. *Int. J. Refract. Met. Hard Mater.* **2017**, *66*, 188–197. [[CrossRef](#)]
11. Kropidlowski, K.; Uhlmann, E.; Woydt, M. Außen-Längs-Runddrehen mit Niobcarbide-Schneidstoff (Straight turning with cutting tools in niobium carbide). *BAM* **2017**, *7–8*, 58–61. (In German)
12. Huang, S.G.; Li, L.; Van der Biest, O.; Vleugels, J. Influence of WC Addition on the Microstructure and Mechanical Properties of NbC-Co Cermets. *J. Alloys Compd.* **2007**, *430*, 158–164. [[CrossRef](#)]
13. Huang, S.G.; Li, L.; Van der Biest, O.; Vleugels, J. VC and Cr₃C₂ doped WC-NbC-Co Hardmetals. *J. Alloys Compd.* **2008**, *464*, 203–209. [[CrossRef](#)]
14. Huang, S.G.; Vanmeensel, K.; Mohrbacher, H.; Woydt, M.; Vleugels, J. Microstructure and Mechanical Properties of NbC-Matrix Hardmetals with Secondary Carbide Addition and Different Metal Binders. *Int. J. Refract. Met. Hard Mater.* **2015**, *48*, 418–426. [[CrossRef](#)]
15. Huang, S.G.; Vleugels, J.; Mohrbacher, H.; Woydt, M. Microstructure and Mechanical Properties of NbC Matrix Cermets Using Ni Containing Metal Binder. *Met. Powder Rep.* **2016**, *71*, 349–355. [[CrossRef](#)]
16. Ramqvist, L. Variation of Hardness, Resistivity, and Lattice Parameter with Carbon Content of Group 5 b Metal Carbides. *Jernkontorets Ann.* **1968**, *152*, 465–475.
17. Vinitskii, I.M. Relation between the properties of groups IV-V transition metals and carbon content. *Powder Metall. Met. Ceram.* **1972**, *11*, 488–493. [[CrossRef](#)]
18. Delanoë, A.; Lay, S. Evolution of the WC Grain Shape in WC-Co Alloys during Sintering: Effect of the C Content. *Int. J. Refract. Met. Hard Mater.* **2009**, *27*, 140–148. [[CrossRef](#)]
19. Zackrisson, J.; André, H.-O. Effect of Carbon Content on the Microstructure and Mechanical Properties of (Ti, W, Ta, Mo)(C, N)-(Co, Ni) Cermets. *Int. J. Refract. Met. Hard Mater.* **1999**, *17*, 265–273. [[CrossRef](#)]
20. Kang, S. Stability of N in Ti(CN) Solid Solutions for Cermet Applications. *Powder Metall.* **1997**, *40*, 139–142. [[CrossRef](#)]
21. Kenneth, C.; Russell, S.Y.; Figueredo, A. Theoretical and Experimental Studies of Ceramic: Metal Wetting. *MRS Bull.* **1991**, *4*, 46–52.
22. Liu, N.; Liu, X.S.; Zhang, X.B. Effect of Carbon Content on the Microstructure and Mechanical Properties of Superfine Ti(C, N)-based Cermets. *Mater. Charact.* **2008**, *59*, 1440–1446. [[CrossRef](#)]
23. Shetty, D.K.; Wright, I.G.; Mincer, P.N.; Clauer, A.H. Indentation Fracture of WC-Co Cermets. *J. Mater. Res.* **1985**, *20*, 1873–1882. [[CrossRef](#)]

24. Warren, R. Carbide Grain Growth During the Liquid-Phase Sintering of the Alloys NbC-Fe, NbC-Ni, and NbC-Co. *J. Less-Common Met.* **1969**, *17*, 65–72. [[CrossRef](#)]
25. Gabriel, S.B.; Brum, M.C.; Candioto, K.C.G.; Sandim, H.R.Z.; Suzuki, P.A.; Nunes, C.A. Kinetics of thermal decomposition of niobium hydride. *Int. J. Refract. Met. Hard Mater.* **2012**, *30*, 38–41. [[CrossRef](#)]
26. Storms, E.K.; Krikorian, N.H. The Variation of Lattice Parameter with Carbon Content of Niobium Carbide. *J. Phys. Chem.* **1959**, *63*, 1747–1749. [[CrossRef](#)]
27. Sundman, B.; Jansson, B.; Andersson, J.O. The Thermo-Calc Databank System. *Calphad* **1985**, *9*, 153–190. [[CrossRef](#)]
28. Lay, S.; Hamar-Thibault, S.; Lackner, A. Location of VC in VC, Cr₃C₂ Codoped WC-Co Cermets by HREM and EELS. *Int. J. Refract. Met. Hard Mater.* **2002**, *20*, 61–69. [[CrossRef](#)]
29. Egami, M.E.; Machida, M. Morphology of Vanadium Carbide in Submicron Hardmetals. In Proceedings of the 13th International Plansee Seminar, Plansee AG, Wattens, Austria, 24–28 May 1993; pp. 639–648.
30. Edwards, R.; Raine, T. The Solid Solubility of Some Stable Carbides in Cobalt Nickel and Iron at 1250 °C. *Pulvermetallurgie Springer-Verlag* **1952**, 232–242.



© 2018 by the authors. Licensee MDPI, Basel, Switzerland. This article is an open access article distributed under the terms and conditions of the Creative Commons Attribution (CC BY) license (<http://creativecommons.org/licenses/by/4.0/>).